Article

Experimental Investigation of the Mechanisms of Salt Precipitation during CO_2 Injection in Sandstone

Yen Adams Sokama-Neuyam [1,2,*] , **Jann Rune Ursin [1]** and **Patrick Boakye [3]**

[1] Department of Energy and Petroleum Engineering, University of Stavanger, NO-4036 Stavanger, Norway; jann-rune.ursin@uis.no

[2] Department of Petroleum Engineering, Kwame Nkrumah University of Science & Technology, UPO, PMB, 00233 Kumasi, Ghana

[3] Department of Chemical Engineering, Kwame Nkrumah University of Science & Technology, UPO, PMB, 00233 Kumasi, Ghana; pboakye3@gmail.com

* Correspondence: yen@petroneer.com; Tel.: +47-925-027-00

check for updates

Abstract: Deep saline reservoirs have the highest volumetric CO_2 storage potential, but drying and salt precipitation during CO_2 injection could severely impair CO_2 injectivity. The physical mechanisms and impact of salt precipitation, especially in the injection area, is still not fully understood. Core-flood experiments were conducted to investigate the mechanisms of external and internal salt precipitation in sandstone rocks. CO_2 Low Salinity Alternating Gas (CO_2-LSWAG) injection as a potential mitigation technique to reduce injectivity impairment induced by salt precipitation was also studied. We found that poor sweep and high brine salinity could increase salt deposition on the surface of the injection area. The results also indicate that the amount of salt precipitated in the dry-out zone does not change significantly during the drying process, as large portion of the precipitated salt accumulate in the injection vicinity. However, the distribution of salt in the dry-out zone was found to change markedly when more CO_2 was injected after salt precipitation. This suggests that CO_2 injectivity impairment induced by salt precipitation is probably dynamic rather than a static process. It was also found that CO_2-LSWAG could improve CO_2 injectivity after salt precipitation. However, below a critical diluent brine salinity, CO_2-LSWAG did not improve injectivity. These findings provide vital understanding of core-scale physical mechanisms of the impact of salt precipitation on CO_2 injectivity in saline reservoirs. The insight gained could be implemented in simulation models to improve the quantification of injectivity losses during CO_2 injection into saline sandstone reservoirs.

Keywords: CO_2 injectivity; salt precipitation; CO_2 storage; drying; impairment

1. Introduction

CO_2 Capture, Utilisation and Storage (CCUS) is a vital mitigation technique to meet the global CO_2 emission reduction target and prevent climate change [1,2]. Adequate storage capacity, a threshold well injectivity and robust containment are prerequisites to a successful CCUS project. Deep saline reservoirs are readily accessible with high volumetric capacity to sequester large volumes of CO_2 [3–6]. However, drying and salt precipitation especially in the injection area could impair CO_2 injectivity in deep saline reservoirs.

Salt precipitation is a well-known flow impairment challenge in natural gas injection and production. Kleinitz et al. [7] reported dramatic halite precipitation around the wellbore during production of natural gas. Similar field cases have been reported during injection, storage and production of gas [8–10]. In terms of field pilots, strong evidence of salt precipitation effects during CO_2 injection

have been reported from the Ketzin reservoir and Snøhvit field [11,12]. Although halite precipitation is common due to the high composition of NaCl in formation water, a case of antarcticite precipitation have been reported by Sminchak et al. [13].

Evidence from laboratory core-flood experiments [14–19] and numerical simulations [20–23] indicate about 13–83% absolute permeability impairment and about 2–15% reduction in porosity. The drying rate, temperature, pressure, solid salt saturation, distribution of precipitated salt in the pore spaces and the petrophysical properties of the reservoir rock are some of the underlying factors of salt precipitation effects [24].

When CO_2 is injected into saline sandstone, water is removed through advection and vaporization [24,25]. As more water is removed from the pore fluid, the concentration of salt in the formation brine increases. When the brine concentration exceeds supersaturation, solid salt drops out into the pores, reducing the flow path [25]. While many researchers have reported adverse effects of salt precipitation especially in the wellbore area [15,16,26], intentional salt clogging is currently been considered as a technique to improve vertical sealing and containment efficiency [27].

Some experimental and numerical studies have in part examined the mechanisms of drying and salt precipitation under CO_2 injection conditions [14,21,28]. From numerical simulation, Hurter et al. [21] reported that the dry-out zone may extend up to 10 m in two years. The mechanisms of drying and salt precipitation include: immiscible two-phase CO_2-brine displacement, brine vaporization, capillary back-flow of brine, diffusion of dissolved, gravity override of displacing CO_2 and salt self-enhancing [24]. Several reports suggests that precipitated salt accumulates near the wellbore where gas flow and brine vaporization are highest [14,15,22,29].

Pruess and Muller [22] suggested that the impact of salt precipitation could be reduced by pre-flushing the damaged zone with freshwater. However, it has been reported that the efficiency of freshwater injection could be reduced if the flow path is plugged with solid salt [7]. In addition, fresh water has a high tendency to react with rock minerals, leading to other injectivity impairment challenges.

The present work investigates the mechanisms and impact of salt precipitation during CO_2 injection into saline sandstone rocks. The effect of drag on precipitated salts and the impact of evolution of the dry-out zone were studied. In addition, CO_2 alternating low salinity water injection (CO_2-LSWAG) as a technique to reduce the impact of precipitated salts on CO_2 injectivity was examined.

2. Materials and Methods

2.1. Materials

Rock Samples: Sandstone core samples, homogeneous in the linear flow direction were used in the experiments (Table 1). Outcrop sandstone rock samples were selected because of their clean and relatively predictable properties. Each core plug has a length of 20 cm long and a diameter of 3.81 cm.

Table 1. Some petrophysical properties of core samples used in the experimental work.

Rock Sample	Brine Permeability (mD)	Porosity (%)
Bentheimer	1600–2400	22–24
Berea	90–105	17–19

The Berea sandstone was used as the primary reservoir rock in the tests due to its suitable range of flow properties. The Bentheimer sandstone rock, was selected because of its high range of permeability.

Brine: Synthetic North Sea formation water (FW), with brine salinity of about 105.5 g/L (NaCl, 77.4 g/L; $CaCl_2 \cdot 2H_2O$, 21.75 g/L; $MgCl_2 \cdot 6H_2O$, 3.56 g/L; $SrCl_2 \cdot 6H_2O$, 2.25 g/L; Na_2SO_4, 0.13 g/L; KCl 0.42 g/L) [30] was used as the main saturating pore water. Dilute solutions of FW were also used in some of the experiments. NaCl brine with salinities of about 150 g/L and 75 g/L were also used as initial saturating brine in some of the tests.

Gas: Liquid CO_2 was used to measure absolute permeability of the cores before and after the tests due to insolubility of the precipitates in CO_2. Supercritical CO_2 obtained by injecting liquid CO_2 at 80 bar and 50 °C was used as the displacing and drying fluid.

2.2. Methods

2.2.1. Experimental Setup

The experimental setup used in the CO_2 core-flood investigations is shown in Figure 1. The cylindrical core sample was horizontally mounted in the hassler core-holder. To measure flow impairment in different sections of the core, the hassler core-holder was replaced with a pressure-tapped core-holder. The Quizix pump and ISCO CO_2 pump delivers brine and liquid CO_2 respectively into a piston cell positioned in the oven to attain a preset temperature. The pressure drop across the core and the pore pressure are monitored in real time through the differential pressure gauge and the pressure transducer. A backpressure of 80 bar is set at the outlet during CO_2 injection. The effluent fluid is collected in a piston cell connected to the backpressure for analysis and safe disposal.
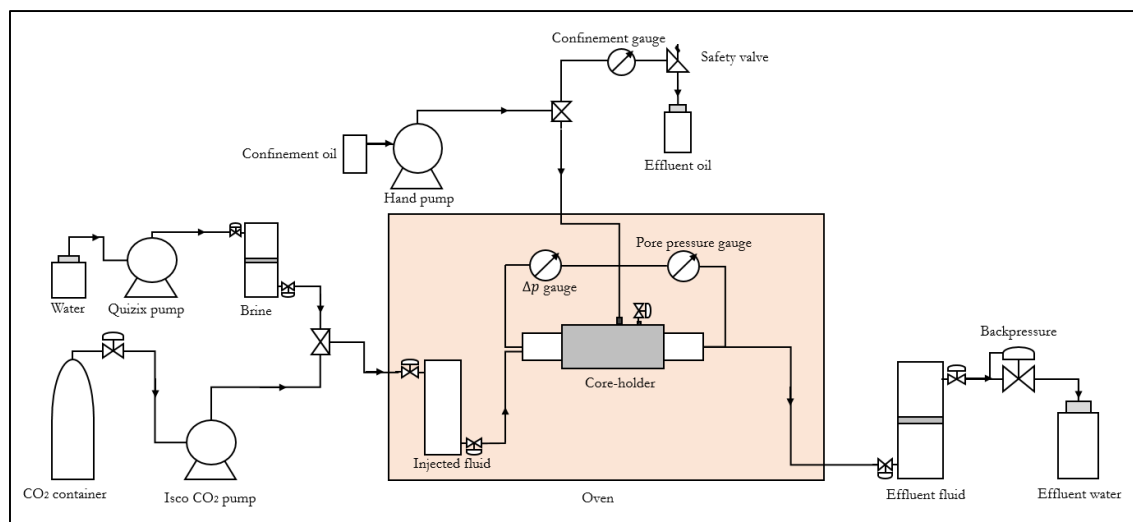

Figure 1. The CO_2 flow rig used for the core-flood tests.

2.2.2. Experimental Procedure

The clean core was initially dried at 65 °C for about 24 h to remove moisture. The core sample was wrapped in shrinking Teflon sleeve to prevent CO_2 leakage before it was inserted into the rubber sleeve in the core holder. A confining pressure of about 20 bar and 150 bar was applied during brine and supercritical CO_2 injection, respectively. Liquid CO_2 was injected into the core at constant injection rate of 5 mL/min to measure its initial permeability. The core was then vacuum saturated with brine and flooded with supercritical CO_2 to dryness. During supercritical CO_2 injection, pressure drop profiles are monitored to analyze the drying process. After drying, when all gaseous CO_2 has bubbled out of the core, liquid CO_2 is injected at 5 mL/min to measure the permeability of the core after exposure to salt precipitation. The initial and final permeability data are analyzed alongside the pressure drop profiles to quantify injectivity impairment.

2.2.3. Theory

For linear flow in a homogeneous core with constant absolute permeability k_i and k_f before and after salt precipitation, respectively, if the viscosity of liquid CO_2 is fairly stable, the injectivity before and after salt accumulation can be expressed from Darcy's law as:

$$I_i = \frac{q_i}{\Delta p_i} = k_i \cdot \eta \tag{1}$$

$$I_f = \frac{q_f}{\Delta p_f} = k_f \cdot \eta \tag{2}$$

where in Equations (1) and (2), η is a constant defined as $\eta = \frac{A}{\mu L}$, for constant cross-sectional area A and length L. If $q_i = q_f$, a relative injectivity change index, β can be defined as:

$$\beta = \left(\frac{I_i - I_f}{I_i} \right) = 1 - \left(\frac{I_f}{I_i} \right) \tag{3}$$

Substituting Equations (1) and (2) into (3) yields:

$$\beta = 1 - \left(\frac{\Delta p_i}{\Delta p_f} \right) = 1 - \left(\frac{k_f}{k_i} \right) \tag{4}$$

Permeability reduction induced by salt precipitation will increase the value of Δp and therefore $\Delta p_f > \Delta p_i$ and $k_i > k_f$ after injectivity impairment. Consequently, β can be used to measure linear changes in CO_2 injectivity at the core-scale. The value of β is often expressed as a percentage.

3. Results

3.1. External Salt Precipitation

During CO_2 injection into fully saturated sandstone core samples, salt may be precipitated onto the surface of the injection inlet in the form of a filter salt cake [15,31]. We investigated the mechanisms of salt deposition in the injection area and identified some underlying parameters.

A clean Bentheimer core was initially vacuum-saturated with 120 g/L NaCl brine. About 100 PV of dry supercritical CO_2 was injected into the brine-filled Bentheimer core at a rate of 1 mL/min. Pressure drop profiles were monitored in real time during CO_2 injection. The core was inspected when an abnormally high pressure drop was detected. Figure 2 shows pictures of the core after the test.

Figure 2. Pictures of Bentheimer sandstone core after CO_2 was injected at 1 mL/min into the core which was initially saturated with 120 g/L NaCl brine. (**A**) No salt cake observed at the core outlet. (**B**) Massive salt cake found at the injection inlet.

Figure 2A shows that no salt was deposited at the core outlet. However, Figure 2B shows massive salt deposition on the core inlet, although the same fittings were used in the inlet and outlet during the test. It was revealed that at the onset of injection, when the core was fully saturated with brine, the injected supercritical CO_2 left brine behind the inlet due to poor sweep. Salinity of the brine increased as water was removed by vaporization. If the initial brine salinity was high enough, the brine left behind the inlet could reach supersaturation and precipitate salt onto the inlet before it was swept into the core. The precipitated salt then created a saturation gradient that drew more brine into the inlet region through capillary backflow, precipitating more salts on the inlet. This suggests that salt

cake deposition on the injection inlet is influenced mainly by brine salinity and sweep efficiency at the core inlet.

To investigate the impact of sweep on external salt deposition, supercritical CO_2 injection rate was increased from 1 mL/min to 5 mL/min. Figure 3 shows that the amount of deposited salts at the injection inlet decreased when the displacing flow rate was increased. Under linear flow conditions, the CO_2—brine sweep improves with increasing injection flow rate. As sweep is improved, less brine is left behind the injection inlet for salt precipitation.

(A) Injection rate: 1 ml/min   (B) Injection rate: 5 ml/min

Figure 3. Pictures showing salt precipitation on the core inlet when supercritical CO_2 injection rate was increased from (**A**) 1 mL/min to (**B**) 5 mL/min. Increase in CO_2 injection rate decreased the amount of deposited salt.

The initial brine salinity was then reduced from 120 to 75 g/L, keeping the CO_2 injection flow rate constant at 5 mL/min to investigate the effect of brine salinity. The amount of salt cake deposited on the injection inlet decreased significantly (Figure 4). At constant vaporization rate, a lower saturating brine salinity delays supersaturation, allowing a significant portion of the brine left behind the injection inlet to be swept into the core.
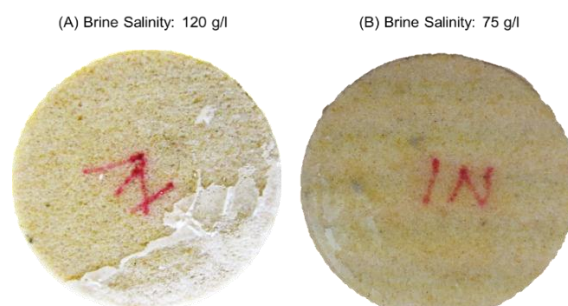
(A) Brine Salinity: 120 g/l   (B) Brine Salinity: 75 g/l

Figure 4. Pictures showing salt cake development at the core inlet when brine salinity was decreased from (**A**) 120 g/L to (**B**) 75 g/L. Decrease in brine salinity further decreased the amount of deposited salts.

3.2. Internal Salt Precipitation

During CO_2 injection into saline sandstone rocks, vaporization of brine may dry the rock and precipitate salt into the dry-out region [18,22,23,32]. As more CO_2 is injected, the dry-out region extends into the rock and the solid salt saturation increases. The effects of drying on CO_2 injectivity, the effect of drag on the distribution of precipitated salt, and evolution of the dry-out region were examined.

A clean Berea core with known initial permeability was saturated with FW. About 300 PV of supercritical CO_2 was injected into the core at a rate of 1 mL/min until the core was completely dried. Under this test conditions, no filter salt cake was detected at the injection inlet. The core permeability after drying was measured and β was calculated. The CO_2 injection flow rate was then increased to 5 mL/min and 10 mL/min, keeping all other parameters constant, to study the effect of injection flow

rate. Figure 5 shows the effect of supercritical CO_2 injection rate on injectivity impairment induced by deposited salts.
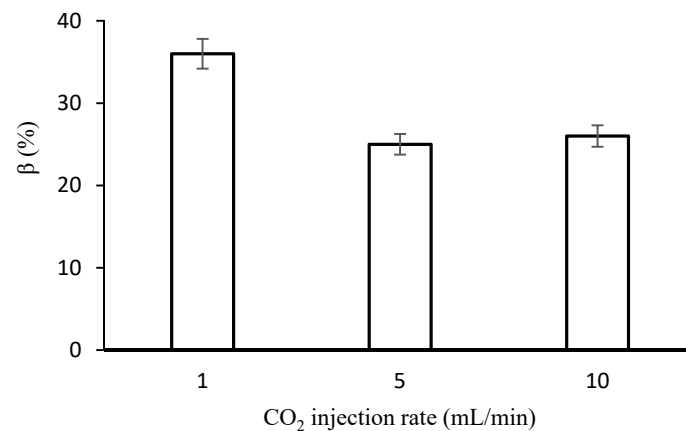

Figure 5. Effect of drying and salt precipitation on CO_2 injectivity. Injectivity impairment, β increased with decreasing CO_2 injection rate.

Figure 5 shows that CO_2 injectivity was impaired by about 36% for a drying rate of 1 mL/min. Injectivity impairment decreased from 36% to about 25% when drying rate was increased to 5 mL/min and remained practically unchanged when the drying rate was further increased to 10 mL/min. Several researchers [17,18,32,33] have reported CO_2 injectivity impairment within a range (13–83%) that agree favorably with the current figures.

At the onset of CO_2 injection, water is removed from the core through advection. Under core-flow conditions, salt precipitation during immiscible CO_2-brine displacement is minimal. At immobile brine saturation, water is removed through vaporization. As more water is removed from the brine, the concentration of salt in the brine increases. When concentration of brine exceed supersaturation, salt precipitates into the pores in the dry-out region as proposed by Zuluaga et al. [25]. The deposited salts reduce the CO_2 flow area, impairing permeability and injectivity. As drying progresses, more brine is drawn into the injection inlet through capillary backflow [24]. The capillary backflow increases with decreasing injection rate.

Injectivity impairment remained practically unchanged when drying rate was further increased from 5 mL/min to 10 mL/min probably because at these injection flow rates, the resident brine was quickly swept out of the core, leaving out only immobile brine for salt precipitation. This suggests that at high injection rates, salt precipitation depends mostly on the immobile brine saturation rather than the drying rate.

3.2.1. Effect of Drag on Precipitated Salt

The effect of drag on deposited salt and its impact on CO_2 injectivity was investigated. A Berea core sample was initially vacuum saturated with FW and vaporized to complete dryness to precipitate salt into the core. Liquid CO_2 permeability of the core was measured and pressure drop across sections of the core were monitored with a pressure-tapped core holder to study the drying process. About 150 PV of supercritical CO_2 was injected into the core at a constant injection rate of 2.5 mL/min. Permeability of the core was then measured after CO_2 flooding and changes in permeability and pressure drop profiles were analyzed. The effect of injection flow rate was investigated by increasing the rate to 5 and 10 mL/min. Figure 6 shows changes in CO_2 permeability induced by drag forces on precipitated salts at varying injection rates.
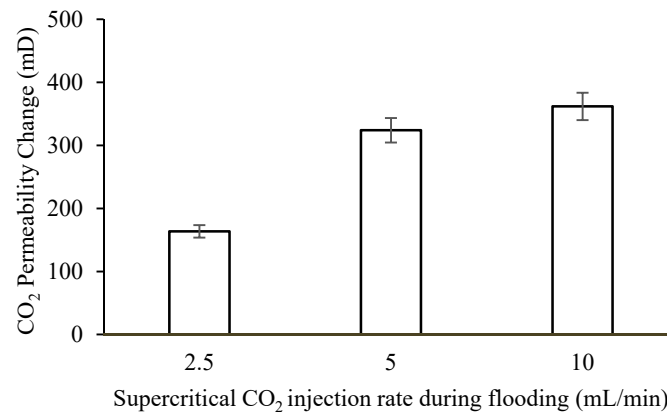
Figure 6. The impact of CO_2 injection flow rate on permeability after salt precipitation. Permeability change is the difference between the core permeability after salt precipitation before drag test and the permeability after drag test.

Generally, the force of drag, F_D experienced by an object is given by [34]:

$$F_D = \frac{1}{2}\rho v^2 C_D A \qquad (5)$$

In Equation (5), ρ is the fluid density, v is the flow rate relative to the object, C_D is the drag coefficient and A is the reference area. From Equation (5), the net drag force exerted by supercritical CO_2 on precipitated salt increases with injection flow velocity (v). The precipitated salts are held to the pore walls mainly by gravitational and electrostatic forces [35]. If drag overcome the attractive forces, the accumulated salts could be dislodged or redistributed in the pores, altering the permeability as a result. The magnitude of permeability change will be proportional to the drag force which in tend depends on the injection flow rate. However, changes in permeability after drag test will be limited by the solid salt saturation. We observed that, for fixed solid salt saturation, there is a maximum change in permeability beyond which further increase in drag cannot produce marked change in permeability. This is probably why no significant permeability change was recorded when injection rate was increased from 5–10 mL/min.

3.2.2. Extension of the Dry-Out Zone

During vaporization, the dry-out region close to the injection inlet extends into the core as more CO_2 is injected [28,32,36]. Core-flood experiments were conducted to study the effect of the advancing dry-out front on CO_2 injectivity. A bundle-of-tubes model was implemented to track the extension of the dry-out zone and estimate the impact of extension of the dry-out region on CO_2 injectivity.

A Berea sandstone core with known initial permeability was saturated with 75 g/L NaCl brine and flooded with supercritical CO_2 at 5 mL/min. The ratio of the advancing dry-out zone to the total length of the core, l_d was estimated after about every 100 PV of CO_2 injection. CO_2 injectivity change as a function of the dry-out length l_d was measured and β computed. To investigate the effect of brine salinity, the experiment was repeated by doubling the brine salinity from 75 g/L (LS) to 150 g/L (HS). Figure 7 shows the impact of the advancing dry-out front, l_d on CO_2 injectivity impairment β.

From Figure 7, CO_2 injectivity impairment was highest at the onset of drying. Injectivity impairment decreased to a minimum at l_d of about 0.45 and then rose slightly as the dry-out zone approached the core effluent end. At the start-up of drying, two mechanisms may be responsible for CO_2 injectivity impairment; salt precipitation and relative permeability effects. Brine vaporization rate is at its highest close to the inlet region where capillary driven back-fluxes are high. As more brine is vaporized, the solid salt saturation in the core increases, which in turn increases flow impairment in this region.

In addition, at the onset of drying, most of the pore spaces are occupied by brine which also reduces the CO_2 relative permeability.
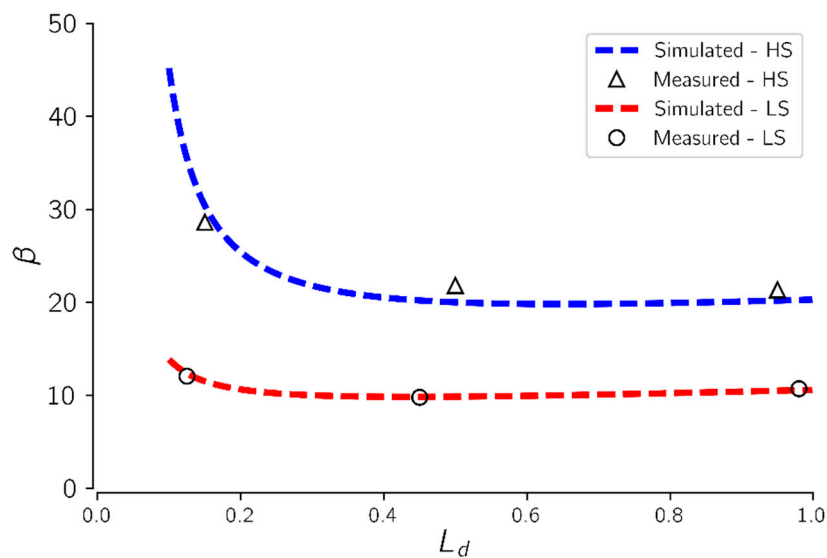

Figure 7. The impact of the dry-out length (L_d) on CO_2 injectivity impairment (β) induced by salt precipitation. Magnitude of injectivity impairment increased when brine salinity was doubled from 75–150 g/L but successive changes in injectivity impairment was not influenced by change in brine salinity.

As the drying front advances into the core, brine vaporization and salt precipitation decreases since most of the brine are drawn into the inlet region by capillary backflow, leaving the remaining section of the core with less brine available for salt precipitation. When the core is almost completely dried, brine vaporization and salt precipitation in and around the effluent end of the core become minimal.

Figure 7 also shows that CO_2 injectivity impairment increased about two-fold when brine salinity was doubled from 75 to 150 g/L at constant injection rate. However, successive changes in CO_2 injectivity impairment as the drying front advances into the core, was not affected by changes in brine salinity. This suggests that the impact of the advancing dry-out zone on CO_2 injectivity is independent of initial brine salinity. Increase in brine salinity increases the magnitude of salt precipitated but the rate of precipitation depends primarily on the brine vaporization rate.

3.3. CO_2 Low Salinity Water Alternating Gas Injection

We investigated CO_2 alternating low salinity water injection as a potential mitigation technique to reduce the impact of salt precipitation on CO_2 injectivity. After salt precipitation, a slug of diluent is injected in attempt to dissolve the precipitated salts, thus temporarily improving CO_2 injectivity. Low salinity water (LSW) prepared by diluting FW was used as the diluent.

A clean Berea core sample was vacuum saturated with FW and aged at 60 °C for 14 days. The aged core was then prepared and flooded with about 50 PV of supercritical CO_2 to vaporize brine and possibly precipitate salts into the pore spaces. After complete dryness, the initial liquid CO_2 permeability of the impaired core was measured. The core was then flushed with about 30 PV of the diluent LSW brine at 0.05 mL/min in attempt to dissolve and wash precipitated minerals after which the core was again vaporized with supercritical CO_2 to complete dryness. Liquid CO_2 pressure drop across the treated core was measured to calculate the final permeability. The permeability data was then used to estimate injectivity improvement. The experiment was repeated by gradually reducing the diluent brine salinity. A theoretical model, developed by Pruess [28] was adapted to simulate expected injectivity improvement induced by dilution of the saturating brine. Figure 8 shows injectivity improvement obtained as a function of mass fraction of salt (X_s) in the diluent.
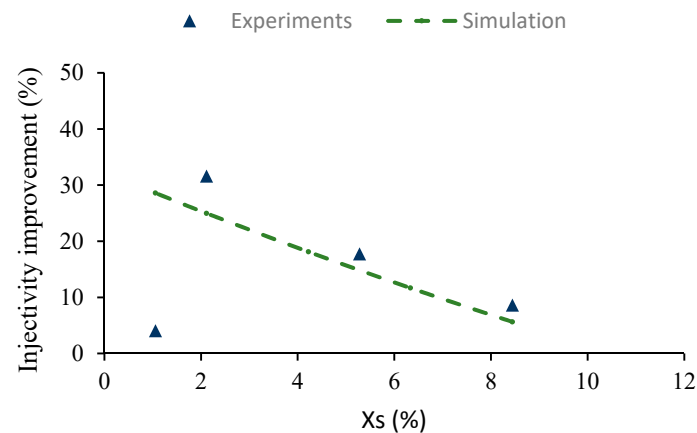
Figure 8. Effect of diluent brine Salinity on CO_2 injectivity after treating the impaired core with CO_2 Low Salinity Alternating Gas (CO_2-LSWAG).

In general, CO_2 injectivity improved from 8.66% to 31.62% when the mass fraction of salt in the diluent, X_s was decreased stepwise from 8.44 to about 2.11 (Figure 8). The solubility of precipitated minerals in the diluent LSW increases with decreasing brine salinity. As the brine is further diluted, more free water molecules become available to interact with precipitated salts.

However, at $X_s = 1.06$, injectivity dropped significantly and the experimental data deviated dramatically from the simulation results, signifying additional injectivity impairment from external mechanisms. At this brine salinity, the diluent starts to interact chemically with the rock minerals. For every sandstone rock, there exist a critical brine salinity below which the diluent will react with the rock minerals [37]. Interaction between rock minerals and the diluent could induce clay swelling and fines mobilization, which could increase CO_2 injectivity impairment.

4. Discussion and Practical Implications

We have examined the mechanisms of salt cake deposition on the surface of the injection inlet and salt precipitation within the dry-out zone. The results indicate that high CO_2 injection flow rate could abate external and internal salt precipitation by improving sweep efficiency at the injection inlet. Increased CO_2 injection rate also reduces capillary backflow of brine which is chiefly responsible for salt precipitation within the dry-out zone.

For fixed initial brine salinity and vaporization rate, the precipitated solid salt saturation is constant. However, the magnitude of CO_2 injectivity impairment is dependent on both solid salt saturation and the distribution of deposited salt within the pore spaces. The results from this study show that continuous injection of CO_2 after salt precipitation could alter the distribution of solid salt and consequently CO_2 injectivity impairment through the action of drag forces on the precipitated salts. This suggests that injectivity impairment induced by salt precipitation should be modelled as a dynamic process rather than a static occurrence.

Pre-flush of the wellbore area with a diluent during CO_2 injection has been shown to be an effective technique to reduce the effect of salt precipitation on CO_2 injectivity. Previously, fresh water was used as the diluent. It could be inferred from this work that fresh water might not be an effective diluent for wellbore pre-flush in sandstone rocks because below a certain critical brine salinity, the diluent can react with the rock minerals to introduce other adverse effects such as clay swelling and fines mobilization. Therefore, for effective treatment of salt impairment, it is suggested that a low salinity brine above the critical brine salinity should be used as the diluent.

It was revealed that the precipitated salt is mainly accumulated in the injection vicinity because of the high fluxes and capillary backflow of brine. Extension of the dry-out zone into the formation as more CO_2 is injected was found to have a negligible impact on CO_2 injectivity impairment induced by salt precipitation. It has been revealed that salt deposition in the dry-out region is not uniform but

rather decreases into the formation as fluxes decreases. Thus, the solid salt saturation is not uniform across the formation after dry-out but also decreases into the formation.

Although only the physical mechanisms of salt precipitation were considered in the study and the results were largely obtained from linear quantifications, the insight gained could improve understanding of pore-scale events before, during and after salt precipitation in saline sandstone rocks. Materials and test conditions were carefully selected to minimize the chemical effects as the main objective was to understand the physical mechanisms of salt precipitation during CO_2 injection into saline reservoirs.

5. Conclusions

Although there are concerns of social acceptability and economic viability, CCUS is considered a plausible technique to reduce CO_2 concentrations in the environment and prevent climate change. To meet global CO_2 emission reduction targets, adequate well injectivity is required to inject large quantities of CO_2. Deep saline aquifers can hold large quantities of injected CO_2 but salt precipitation during CO_2 injection could impair injectivity and reduce their quality for CO_2 storage.

Core-flood experiments were conducted to investigate the physical mechanisms of salt precipitation during CO_2 injection into saline sandstone rocks. The mechanisms of external and internal salt precipitation, the drying process and post-precipitation effects were investigated. Also, alternate injection of CO_2 and low salinity water as a potential mitigation technique was tested. Some highlights of the work include the following:

- Poor sweep and high brine salinity are strong controlling parameters of external salt precipitation on the surface of the injection area.
- Salt precipitation-induced injectivity impairment could be a dynamic process. Injectivity impairment depends on both the solid salt saturation which is generally static and the distribution of precipitated salt in the pore spaces which is a dynamic process.
- Alternate injection of CO_2 and low salinity brine could reduce the effect of salt precipitation on CO_2 injectivity. However, below a certain diluent brine salinity, CO_2–LSWAG might not improve injectivity.

The findings improve understanding of the physical mechanisms of salt precipitation during CO_2 injection into fully saturated sandstone rocks. The findings serve as valuable foundation for improving CO_2 injectivity in deep saline reservoirs and could be implemented to improve the quantification of injectivity losses during CO_2 injection into brine-saturated sandstone rocks.

References

1.　Baena-Moreno, F.M.; Rodríguez-Galán, M.; Vega, F.; Alonso-Fariñas, B.; Vilches Arenas, L.F.; Navarrete, B. Carbon capture and utilization technologies: A literature review and recent advances. *Energy Sources Part A Recovery Util. Environ. Eff.* **2018**, 1–31. [CrossRef]
2.　Cuéllar-Franca, R.M.; Azapagic, A. Carbon capture, storage and utilisation technologies: A critical analysis and comparison of their life cycle environmental impacts. *J. CO2 Util.* **2015**, *9*, 82–102. [CrossRef]
3.　Holloway, S. Storage of fossil fuel-derived carbon dioxide beneath the surface of the earth. *Annu. Rev. Energy Environ.* **2001**, *26*, 145–166. [CrossRef]

4. Gunter, W.D.; Wong, S.; Cheel, D.B.; Sjostrom, G. Large CO_2 sinks: Their role in the mitigation of greenhouse gases from an international, national (Canadian) and provincial (Alberta) perspective. *Appl. Energy* **1998**, *61*, 209–227. [CrossRef]

5. Baines, S.J.; Worden, R.H.; Jackson, R.E. *Geological Storage of Carbon Dioxide*; The Geological Society: London, UK, 2009; Volume XV, pp. 115–116.

6. Li, L.; Zhao, N.; Wei, W.; Sun, Y. A review of research progress on CO_2 capture, storage, and utilization in Chinese Academy of Sciences. *Fuel* **2013**, *108*, 112–130. [CrossRef]

7. Kleinitz, W.; Dietzsch, G.; Köhler, M. Halite scale formation in gas-producing wells. *Chem. Eng. Res. Des.* **2003**, *81*, 352–358. [CrossRef]

8. Golghanddashti, H.; Saadat, M.; Abbasi, S.; Shahrabadi, A. Experimental investigation of water vaporization and its induced formation damage associated with underground gas storage. *J. Porous Media* **2013**, *16*, 89–96. [CrossRef]

9. Jasinski, R.; Sablerolle, W.; Amory, M. ETAP: Scale Prediction and Contol for the Heron Cluster. In Proceedings of the SPE Annual Technical Conference and Exhibition, San Antonio, TX, USA, 5–8 October 1997; Society of Petroleum Engineers: Houston, TX, USA, 1999.

10. Place, M.C., Jr.; Smith, J. An Unusual Case of Salt Plugging in a High-Pressure Sour Gas Well. In Proceedings of the 59th Annual Technical Conference and Exhibition, Houston, TX, USA, 16–19 September 1984; SPE, Ed.; Society of Petroleum Engineers: Houston, TX, USA, 1984; p. 13. [CrossRef]

11. Baumann, G.; Henninges, J.; De Lucia, M. Monitoring of saturation changes and salt precipitation during CO_2 injection using pulsed neutron-gamma logging at the Ketzin pilot site. *Int. J. Greenh. Gas Control* **2014**, *28*, 134–146. [CrossRef]

12. Grude, S.; Landrø, M.; Dvorkin, J. Pressure effects caused by CO_2 injection in the Tubåen Fm., the Snøhvit field. *Int. J. Greenh. Gas Control* **2014**, *27*, 178–187. [CrossRef]

13. Sminchak, J.; Zeller, E.; Bhattacharya, I. Analysis of unusual scale build-up in a CO_2 injection well for a pilot-scale CO_2 storage demonstration project. *Greenh. Gases Sci. Technol.* **2014**, *4*, 357–366. [CrossRef]

14. Peysson, Y.; André, L.; Azaroual, M. Well injectivity during CO_2 storage operations in deep saline aquifers-Part 1: Experimental investigation of drying effects, salt precipitation and capillary forces. *Int. J. Greenh. Gas Control* **2014**, *22*, 291–300. [CrossRef]

15. Bacci, G.; Korre, A.; Durucan, S. Experimental investigation into salt precipitation during CO_2 injection in saline aquifers. *Energy Procedia* **2011**, *4*, 4450–4456. [CrossRef]

16. Kim, M.; Sell, A.; Sinton, D. Aquifer-on-a-Chip: understanding pore-scale salt precipitation dynamics during CO_2 sequestration. *Lab. Chip* **2013**, *13*, 2508–2518. [CrossRef]

17. Muller, N.; Qi, R.; Mackie, E.; Pruess, K.; Blunt, M.J. CO_2 injection impairment due to halite precipitation. *Energy Procedia* **2009**, *1*, 3507–3514. [CrossRef]

18. Tang, Y.; Yang, R.; Du, Z.; Zeng, F. Experimental study of formation damage caused by complete water vaporization and salt precipitation in sandstone reservoirs. *Transp. Porous Media* **2015**, *107*, 205–218. [CrossRef]

19. Sokama-Neuyam, Y.A.A.; Ursin, J.R. The Effect of Mineral Deposition on CO_2 Well Injectivity. In Proceedings of the EUROPEC 2015, Madrid, Spain, 1–4 June 2015.

20. Giorgis, T.; Carpita, M.; Battistelli, A. 2D modeling of salt precipitation during the injection of dry CO_2 in a depleted gas reservoir. *Energy Convers. Manag.* **2007**, *48*, 1816–1826. [CrossRef]

21. Hurter, S.; Berge, J.; Labregere, D. Simulations for CO_2 injection projects with Compositional Simulator. In Proceedings of the Offshore Europe, Aberdeen, Scotland, UK, 4–7 September 2007. [CrossRef]

22. Pruess, K.; Muller, N. Formation dry-out from CO_2 injection into saline aquifers: 1. effects of solids precipitation and their mitigation. *Water Resour. Res.* **2009**, *45*, 1–11. [CrossRef]

23. Zeidouni, M.; Pooladi-Darvish, M.; Keith, D. Analytical solution to evaluate salt precipitation during CO_2 injection in saline aquifers. *Int. J. Greenh. Gas Control* **2009**, *3*, 600–611. [CrossRef]

24. Miri, R.; Hellevang, H. Salt precipitation during CO_2 storage—A review. *Int. J. Greenh. Gas Control* **2016**, *51*, 136–147. [CrossRef]

25. Zuluaga, E.; Muñoz, N.I.; Obando, G.A. An Experimental Study to Evaluate Water Vaporisation and Formation Damage Caused by Dry Gas Flow Through Porous Media. In Proceedings of the International Symposium on Oilfield Scale, Aberdeen, UK, 30–31 January 2001.

26. Miri, R.; van Noort, R.; Aagaard, P.; Hellevang, H. New insights on the physics of salt precipitation during injection of CO_2 into saline aquifers. *Int. J. Greenh. Gas Control* **2015**, *43*, 10–21. [CrossRef]

27. Wasch, L.J.; Wollenweber, J.; Tambach, T.J. Intentional salt clogging: A novel concept for long-term CO_2 sealing. *Greenh. Gases Sci. Technol.* **2013**, *3*, 491–502. [CrossRef]

28. Pruess, K. Formation dry-out from CO_2 injection into saline aquifers: 2. analytical model for salt precipitation. *Water Resour. Res.* **2009**, *45*, 1–6. [CrossRef]

29. Kleinitz, W.; Koehler, M.; Dietzsch, G.; Gmbh, P.E. The precipitation of salt in gas producing wells. In Proceedings of the SPE European Formation Damage Conference, The Hague, The Netherlands, 21–22 May 2001; SPE, Ed.; SPE: The Hague, The Netherlands, 2001; pp. 1–7. [CrossRef]

30. Fjelde, I.; Omekeh, A.V.A.V.; Sokama-Neuyam, Y.A.Y.A. Low Salinity Water Flooding: Effect of Crude Oil Composition. In Proceedings of the SPE Improved Oil Recovery Symposium, Tulsa, OK, USA, 12–16 April 2014. [CrossRef]

31. Jeddizahed, J.; Rostami, B. Experimental investigation of injectivity alteration due to salt precipitation during CO_2 sequestration in saline aquifers. *Adv. Water Resour.* **2016**, *96*, 23–33. [CrossRef]

32. Peysson, Y. Permeability alteration induced by drying of brines in porous media. *Eur. Phys. J. Appl. Phys.* **2012**, *60*, 12. [CrossRef]

33. Bacci, G.; Durucan, S.; Korre, A. Experimental and Numerical Study of the Effects of Halite Scaling on Injectivity and Seal Performance During CO_2 Injection in Saline Aquifers. *Energy Procedia* **2013**, *37*, 3275–3282. [CrossRef]

34. Batchelor, G.K. *An Introduction to Fluid Dynamics*; Cambridge University Press: Cambridge, UK, 2000.

35. Khilar, K.C.; Fogler, H.S. *Migrations of Fines in Porous Media*; Springer Science & Business Media: Berlin, Germany, 1998; Volume 12.

36. Prat, M. Recent advances in pore-scale models for drying of porous media. *Chem. Eng. J.* **2002**, *86*, 153–164. [CrossRef]

37. Khilar, K.; Fogler, H. The existence of a critical salt concentration for particle release. *J. Colloid Interface Sci.* **1984**, *101*, 214–224. [CrossRef]